High-Temperature Performance Evaluation of a Novel Graphene-Based Aerogel

B Mourched[1]*, N Abboud[2], M Abdallah[2]

1. College of Engineering and Technology, American University of the Middle East, Egaila 54200, Kuwait

2. Faculty of Science, Lebanese University, Lebanon

ABSTRACT

This paper provides an in-depth analysis of the thermal and mechanical properties of Ethylenediamine Graphene Aerogel (EGA) using COMSOL Multiphysics software. The study focuses on understanding the stress distribution and mechanical responses of this material under various conditions. Thermal stress applied to the bottom of a cylindrical structure revealed distinct stress patterns over time and temperature. High-stress regions were noted towards the cylinder's center, suggesting the effects of temperature fluctuations, while the upper surface experienced lower stress. The von Mises stress increased over time, indicating the material's response to heat, particularly near the heat source, and stabilized around 40 minutes, suggesting a new thermal equilibrium. A critical observation was made at a critical region from the cylinder's bottom, where a significant shift in stress patterns and performance characteristics occurred, emphasizing the need to consider these variations in design for safety and functionality. This study highlights the material's low thermal conductivity and its role in temperature distribution, demonstrating its capability to manage thermal expansion effectively. These properties make the Ethylenediamine Graphene Aerogel suitable for high-temperature applications such as aerospace, automotive, and thermal barrier systems, and open avenues for further applications.

1. INTRODUCTION

The dawn of the 21st century brought forth a wave of Nano-technological marvels. At the vanguard of this revolution stood graphene, an atomic-scale hexagonal lattice made of flat monolayers of carbon atoms. Its discovery was not just another addition to the annals of science, but a watershed moment that promised to reshape industries. Revered for its unparalleled electrical conductivity, high heat resistance, and unmatched mechanical strength [1], [2], graphene soon became the cynosure of the scientific community. With an ultrahigh Young's modulus, outstanding elasticity, and zero bandgap, graphene stands as the universe's lightest and thinnest material, boasting an optical transmittance of over 98% [3].

Graphene's extraordinary properties have paved the way for various applications, such as advanced thermal conductors, supercapacitor electrodes, high-speed transistors, and sensors [4], [5]. Biochemical and chemical sensors, hydrogen storage [6], energy storage in solar cells [7], biomedicine, and automotive are some of the other possible application areas [8], [9]. However, the single component graphene material has certain limitations, such as weak electrochemical activity, easy agglomeration into graphite-like powders, and difficult

*Corresponding Author: bachar.mourched@aum.edu.kw

processing, which greatly limit the applications of graphene and its practicality. Therefore, functional modification of graphene and graphene oxide is crucial to expanding their applications. The functionalization of graphene and graphene oxide is based on the further modification of their intrinsic structure. To harness its unique properties effectively, researchers have explored the self-assembly of graphene sheets into three-dimensional structures like hydrogels and aerogels, which offer both micro and mesoporous networks. Each of these graphene derivatives has its attributes and potential applications.

Aerogels are among the world's lightest materials. They are synthetic materials made from wet gels in which the liquid has been replaced by air [10]. Aerogels and their composites of various types have been proposed for CO2 capture, oil-water separation, volatile organic compound adsorption, organic dye pollutants, and heavy metal ion adsorption due to their chemical stability, low density, high porosity, high specific surface area, and adaptive surface chemistry [11]. Aerogels, known for their low density and high porosity, found an enhanced efficacy when combined with the robustness of graphene. The graphene aerogels (GAs) exhibit remarkable properties, including lightweight structure [12], [13], large surface areas [14], high electrical and thermal conductivity [15], excellent compressibility [16]–[18], recoverability [19], and thermal insulation [20]. These qualities make GAs promising materials for wide variety of applications such as in catalysis, energy storage, actuators, supercapacitors, high quality electrodes, air purification, the absorption of several oils and dyes from water, waste water treatments (removal of volatile organic compounds, metal contaminants and dyes, etc.) and environmental protection and remediation [21]–[24]. GAs are among the most important materials for adsorption-based treatment of oily wastewater. GAs are superior to old-fashioned one-dimensional and two-dimensional adsorption materials due to their high adsorption capacity and excellent durability, allowing them to be regenerated by extrusion [25].

2. NITROGEN-DOPED GRAPHENE AEROGELS

A recent research work [26] proposed a one-step hydrothermal synthesis method to create Nitrogen-doped Graphene Aerogels for water decontamination addressing groundwater pollution issues caused by leakage from oil reservoirs, gas stations, and pipelines causing significant environmental and health risks [27]. In their work, three-dimensional nitrogen-doped graphene aerogels were produced in an easy and efficient manner using a one-step hydrothermal reduction of graphene oxide, which was mixed with a few drops of ethylenediamine, then freeze-dried for 24h. They have successfully synthesized an Ethylenediamine Graphene Aerogel (EGA) with an exceptionally low density of 15 mg.cm-3, by adjusting various process parameters such as changing the hydrothermal treatment periods, gelation time, temperature, freezing temperature, drying pressure, and the solvent choice. This EGA exhibits an ultralow thermal conductivity (~ 0.056 $W.m^{-1}.K^{-1}$), a highly favorable attribute in water purification, boasting an impressive adsorption capacity of 41 g/g, surpassing the performance of most other Graphene Aerogel toluene adsorbents.

Detailed empirical analyses has invaluable insights into the EGA depth understanding and becomes pivotal when one envisions its application in diverse sectors, from environmental purification to advanced energy storage solutions and engineering applications. Thus, it is of utmost importance to explore the thermal and mechanical behavior of the EGA material as they are crucial factors in engineering applications. In engineering applications that require materials to withstand high thermal stress, it is essential that the material can accommodate

thermal expansion without leading to excessive pressure buildup. A material that maintains lower pressure values at elevated temperatures is indicative of good thermal expansion management, which is crucial for applications like aerospace components, automotive parts, and thermal barrier systems. While empirical data provides a robust foundation, the dynamic nature of scientific inquiry necessitates a foray into predictive analytics. Simulations, in this context, become invaluable. This paper seeks to not only highlight these experimental outcomes but also extend understanding through state-of-the-art simulations using COMSOL Multiphysics. The focus will be to evaluate pressure and stress distributions across an EGA based cylindrical design. The endeavor bridges experimental data with simulation insights, pushing boundaries in the application of EGAs across sectors ranging from environmental purification to advanced energy storage solutions. Thus, we are using the values of the measured parameters of the EGA in order to analyze and investigate the thermal and mechanical stress behavior of an EGA-based cylindrical geometry conducted by a powerful simulation tool, COMSOL Multiphysics. COMSOL is a Finite Element analysis software designed to solve various physical problems described by differential equations in a variety of fields such as optical, electrical, thermal, and mechanical applications [27]–[34], and combined with machine learning studies for sustainable applications [35]–[39]. These simulations, while grounded in the empirical, venture into the realm of the predictive, offering insights that could shape the future applications of EGAs.

In the following sections, we will delve deeper into the key concepts required to understand this study, present the design and methods employed, and discuss the results and conclusions of our investigation. The first section is dedicated to presenting the structure design through COMSOL Multiphysics and studying the internal thermal distribution within the EGA. By manipulating variables such as thermal conductivity and temperature gradients, we seek a detailed understanding of how the graphene-based structure influences heat dissipation and distribution. The second section delves into the mechanical responses of these aerogels under various stresses. Analyzing deformations, stresses, and behaviors in response to external forces sheds light on the mechanical strength and flexibility of these structures. By merging the results from thermal and mechanical studies, we gain a holistic perspective on the performance of the graphene-based aerogels. This multidisciplinary approach provides an in-depth insight that can be valuable for applications ranging from advanced thermal insulation materials to lightweight and durable mechanical devices.

3. SIMULATION DESIGN AND STUDY

The analyzed sample used in this study is a simple 3D cylindrical geometry made of EGA material, defined in vertical position. It has a radius of 0.015 mm and a length of 0.025 mm. These dimensions closely mirror the authentic sizes of heat-sensitive electronic devices that our paper intends to investigate. 3D models can better capture the coupling between phenomena such as heat transfer and stress distribution to accurately account for the convective effects in all directions. This numerical study incorporates two different physics interfaces, solid mechanics, and heat transfer, in a dynamic context where conditions change over time. COMSOL is generating an interface node combining these two studies and illustrating how these phenomena interact over time. In the solid mechanics study, the structure boundaries are defined to study the deformation or motion of solids under external applied loadings including forces, displacements, temperature changes, or other agents.

This study is using the equation of motion stating that the divergence of stress equals the volume force (equation 1),

$$0 = \nabla . FS + Fv \tag{1}$$

where FS is the deformation gradient (1st Piola-Kirchhoff stress), S is the stress (2nd Piola-Kirchhoff stress), and Fv is the volume force.

The heat transfer study is employed to examine the effects of heating and cooling on devices and processes. It encompasses simulation tools for modeling all forms of heat transfer, such as conduction, convection, and radiation (equation 2),

$$\rho A C_p \frac{\partial T}{\partial t} + \rho A C_p \, u . \nabla T = \nabla . A \, k \, \nabla T + f_D \frac{\rho A}{2 d_h} |u|^3 + Q + Q_{wall} + Q_p \tag{2}$$

where ρ is the fluid density, A is the pipe cross section area available for flow, C_p is the heat capacity at constant pressure, T is the temperature, u is a velocity field, k is the thermal conductivity. The second term on the right-hand side corresponds to friction heat dissipated due to viscous shear. Q is a general heat source and Q_{wall} is an external heat exchange.

Properties of the EGA material, derived from experimental findings, are incorporated into the COMSOL analysis as presented in Table 1.

Table 1. EGA Material Properties

Properties (units)	Values
Coefficient of thermal expansion (1/k)	1.2
Heat capacity at constant pressure (J/(kg·k))	1800
Thermal conductivity (w/(m·k))	0.056
Density (kg/m³)	22
Young's modulus (Pa)	21×10^3
Hole mobility (in bulk) (cm^2/V s)	450

To numerically solve the differential equations used in each interface used, the model requires spatial discretization in the form of a mesh. The mesh subdivides the domain into smaller elements, enabling the equations to be solved at mesh points to obtain an approximation of the different required outcomes such as temperature or stress distribution throughout the material. Figure 1 represents an extremely fine tetrahedral meshing model.

The bottom surface of the cylinder is defined as a heat source of temperature T, and the rest of the structure is exposed to ambient temperature. To evaluate the effect of temperature on the EGA material, we are visualizing the stress distribution throughout the structure in terms of time and for different temperatures.

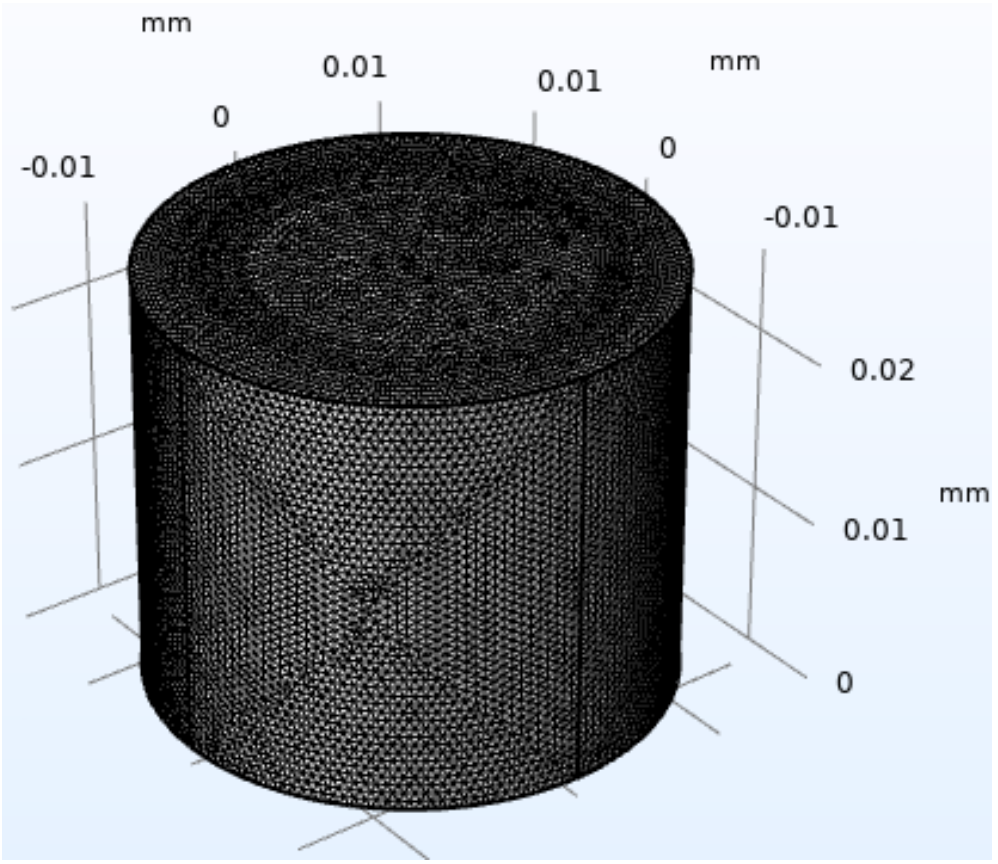

Fig. 1. An extremely fine tetrahedral meshing model for the cylindrical structure

3.1. Stress distribution

The pressure variations are directly correlated with the heating temperatures applied to the lower surface of the graphene-based aerogel cylinder. An increase in temperature leads to thermal expansion of the material, resulting in pressure variations. This analysis underscores the importance of understanding the interactions between temperature, thermal expansion, and mechanical stresses in assessing the material's behavior under changing thermal conditions. In the context of the stress analysis of the EGA material, the von Mises equivalent stress measurement allows a simplified representation of the various stresses acting on a point in the material. First, we are pointing out a visual representation of the stress distribution through the design made by EGA material over three different times: at t = 0 minutes, t = 20 minutes, and t = 40 minutes (figure 2). This allows visualizing and tracking the evolution of the material behavior under thermal stress.

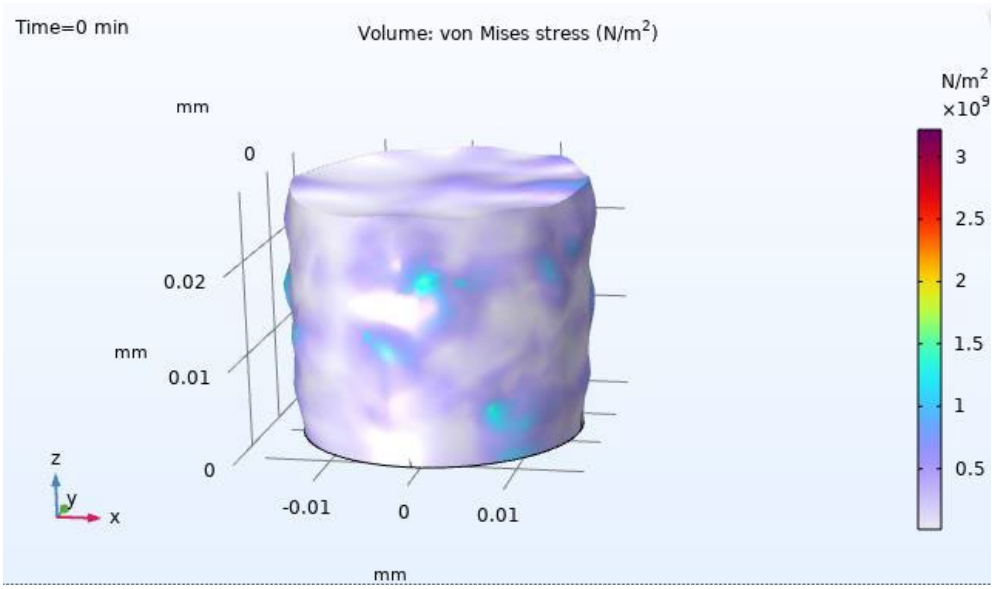

a) at t = 0 minutes

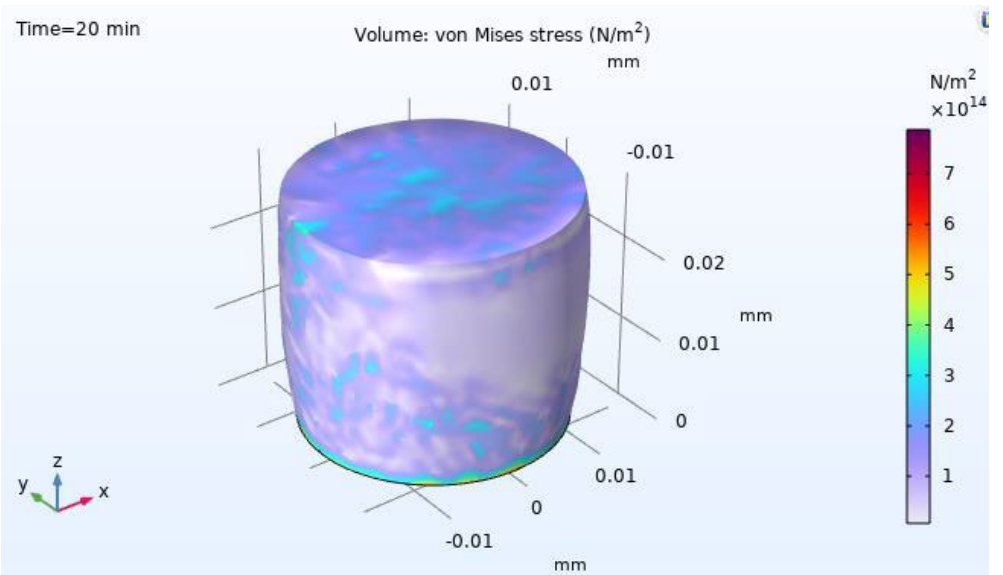

b) at t = 20 minutes

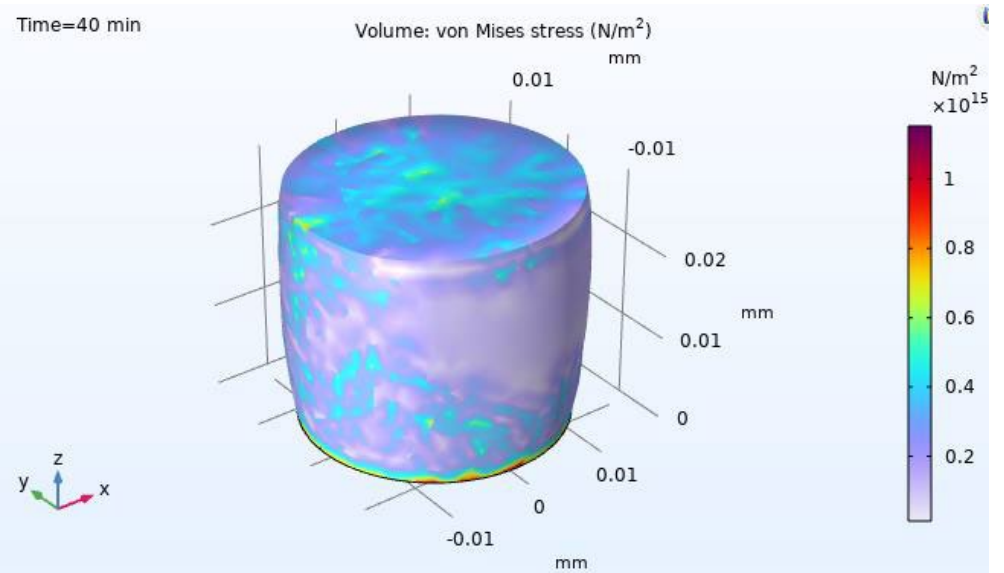

c) at t = 40 minutes

Fig. 2. Von-mises stress distribution through the EGA structure for three different time, a) at t = 0 minutes, b) at t = 20 minutes, and c) at t = 40 minutes

At t= 0 minutes (figure 2.a), The Von Mises stress is mostly uniform across the object, with the color gradient indicating minimal stress. The scale shows that the stress values are very low, which suggests that either the thermal conditions have just started to be applied, resulting in an almost unstressed state, or the material has a high resistance to thermal stress at this initial temperature. After 20 minutes (figure 2.b), there are noticeable changes in the stress distribution. The scale on the right side indicates higher stress values compared to the initial state, with some areas experiencing significantly higher stress located at the bottom surface. The increase in stress values (from blue/green to yellow/red zones) indicates that the heat has penetrated further into the material, creating a thermal gradient through its thickness. This gradient induces thermal stress due to differential expansion between the heated bottom and the cooler top surface. This could be justified, as the thermal gradient is greatest near the heat source indicating that the material is undergoing thermal expansion and starting to experience moderate thermal stress. The stress pattern shows that the material has regions with different thermal expansion coefficients or varying constraints that affect how the stress is distributed. The image representing 40 minutes interval (figure 2.c) shows a noticeable shift in the distribution of von Mises stress and higher values compared to the image at t=20 minutes. The distribution of stress has become more pronounced and varied across the surface, with a wider range of colors indicating a complex pattern of stress distribution. The highest stress regions in red color have become more localized, potentially indicating regions of maximum thermal expansion, which could imply that the material is nearing a point of failure or that it is undergoing a deformation in those regions. These areas are likely closest to the heat source or are where thermal expansion is most resisted, either by the material's constraints

or by a temperature gradient that is steep enough to cause significant stress. This could be due to several factors including material inhomogeneities, variations in thermal conductivity, or geometric constraints that prevent uniform expansion.

As conclusion, the stress distribution over time is not uniform and is increasing over time due to thermal expansion. The stress pattern at 40 minutes, with its localized high-stress regions, indicates that the material might be experiencing thermal fatigue or nearing a point where thermal creep could become significant, depending on the material properties and the duration of exposure to the thermal load. Thus, the material could be approaching its thermal stress limits, which might lead to failure if the stress exceeds the material's yield strength. Alternatively, if the system is designed to reach a thermal equilibrium, we might expect the stress distribution to stabilize over time as the material adapts to the temperature change and the expansion is accommodated within the structure.

To investigate more about the EGA material behavior over thermal stress, we measured the Von-mises stress through the arc length of the cylinder in order to see to the maximum values of stress reached in different regions in the structure for different temperatures. "Arc length (mm)" refers to the measurement taken along the central axis of the cylinder, extending from the bottom to the top surface, amounting to a total length of 0.025 mm. The figure 3 illustrates the von Mises stress measurement along the arc length of the cylinder for three different temperatures: 303.15 K,333.15 K, and 363.15 K.

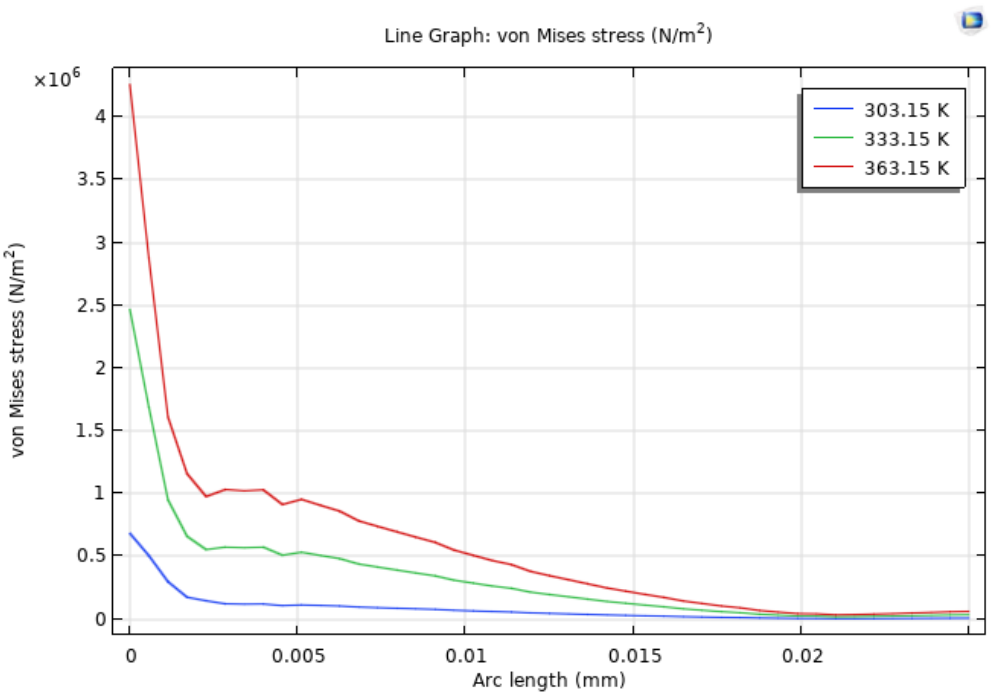

Fig. 3. Von-mises stress measurement throughout the structure at three different temperatures

One can observe that the stress is showing highest values at the bottom surface of the cylinder. This is valid for the three different temperatures. However, the highest stress value is 4.7 N/m^2 measured at 363 K, followed by a 2.5 N/m^2 stress at 333 K, and 0.6 N/m^2 stress at 303 K. This indicates that the immediate response of the material to heating is to develop a significant thermal stress, likely due to thermal expansion being constrained by the material or by the boundaries of the cylinder. Beyond a certain point (just after 0.005 mm), the stress values for the three temperatures converge, indicating that the effect of temperature on stress becomes less significant along the rest of the arc length. As we move from the heated bottom surface across the cylinder towards its top surface (0.025 mm), the stress values for all temperatures decrease, reflecting a gradient of thermal stress across the height of the cylinder. This gradient is steeper for higher temperatures, as shown by the red (T=363 K) line descending more steeply than the blue line (T=303 K). As the distance from the heat source increases, the stress values for all three temperatures converge and eventually stabilize towards a lower value near the top surface of the cylinder (0.025 mm), which deduce that the temperature effect diminishes with distance from the heat source and stress values stabilize, affirming the transmission of stresses through the EGA material. Near the top surface, the stress for all three temperatures is lower and approaches a similar value, which could indicate that the effect of the initial temperature differential is mitigated at the top due to either less material constraint or due to the material reaching a uniform temperature along the height of the cylinder. The convergence of stress values near the top suggests a reduction in the temperature gradient and a more uniform distribution of thermal expansion.

3.2. Pressure analysis

Understanding the pressure distribution is also critical for judging the suitability of the material for high thermal stress applications. Materials with high thermal expansion coefficients or low thermal conductivity could develop significant internal pressures when subjected to thermal gradients, potentially leading to failure. The ability of a material to withstand these pressures without yielding or fracturing is crucial in applications such as pressure vessels, engines, or other engineering applications and components exposed to high temperatures. Figure 4 provides the Gauss point evaluation pressure of the EGA material across the arc length of the cylinder, which indicates how the material behaves under thermal stress.

One can figure out that the initial high-pressure readings at the bottom surface of the cylinder, at the highest temperature of 363.15 K, suggest a strong thermal expansion at the heat source. Thermal expansion is likely exerting force against the material's constraints, creating compressive stress that translates into higher pressure. Likely for the case of 333.15 K and 303.15 K, the Gauss point evaluation pressure values are the highest at the cylinder bottom surface. The steep decline in pressure along the arc length, especially pronounced at 363.15 K indicates that the material's thermal expansion decreases with distance from the heat source. The rapid decrease implies that the expansion-induced pressure is highly localized near the bottom surface where the temperature is highest. This is consistent with the principle that materials typically expand more at higher temperatures if the expansion is not uniform due to temperature gradients within the material. A critical point at approximately 0.005 mm where the three lines intersect, and flip is particularly interesting. This point represents a location along the arc length where the pressure measurements for all three temperatures are equal, despite the different initial temperatures at the heat source. At this special region from

the cylinder bottom surface, the material's response to thermal expansion is uniform across all three temperatures. After the intersection point, the lines flip, indicating that material could undergo a change in its expansion behavior due to phase transitions or other thermal effects, which could result in less expansion and therefore lower pressure. At this critical region, the thermal gradient may also have become more uniform across the cylinder, reducing the differential expansion that would lead to higher pressures. Then, the convergence of pressure values for all temperatures diminishes to near-zero levels as we approach the top surface of the cylinder (0.025 mm). This could mean that the temperature throughout the material becomes steadier away from the heat source, reducing thermal gradients and therefore reducing expansion-related pressure.

In conclusion, based on the analysis provided in the figures 2 and 3, it is important to highlight the change in behavior of the Von-mises stress and the Gauss point evaluation at a critical region near a distance of 0.005 mm away from the cylinder bottom surface. This region could have significant implications on the material behavior and suggests a complex interaction between temperature, material properties, and perhaps structural constraints. It indicates a temperature range where the material's performance changes, which must be accounted for in design considerations, and therefore, this behavior must be considered to ensure that designs can accommodate such variations without compromising safety or functionality.

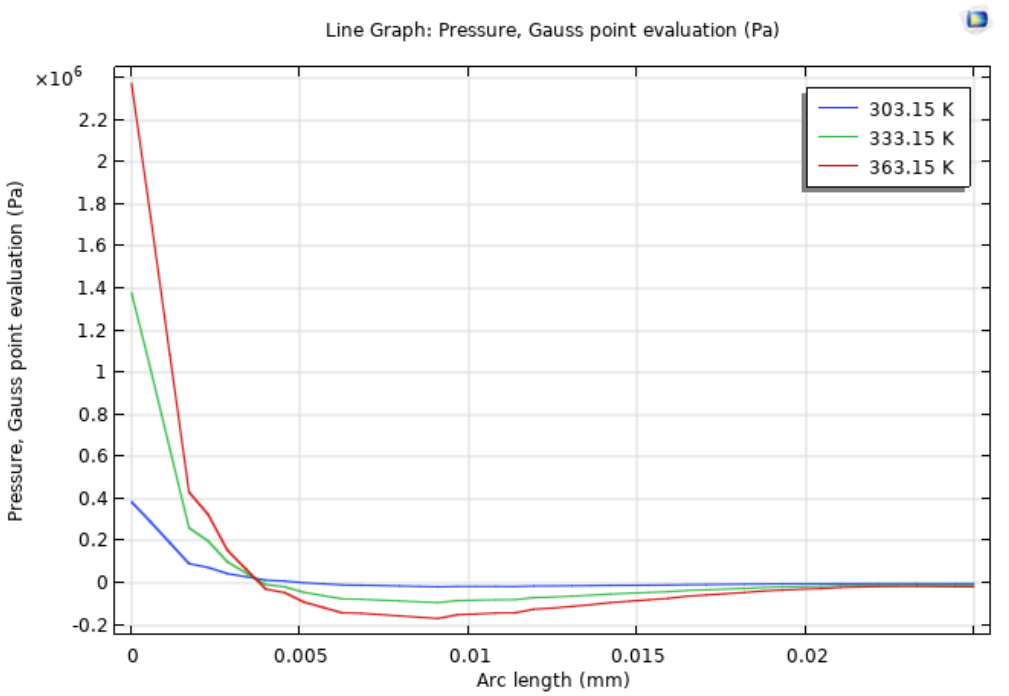

Fig. 4. Gauss point evaluation pressure measurement across the cylinder arc length for three different temperatures.

4. DISCUSSION

The substantial shift in stress patterns and performance characteristics observed at the specific region from the cylinder's bottom surface, as aforementioned, can be understood through several contextual and analytical lenses:

- Thermal gradient and material response: As the temperature increases, especially near the heat source at the cylinder's bottom, a thermal gradient is established. The intense thermal gradient at the bottom causes different parts of the material to expand at varying rates. This differential expansion leads to non-uniform stress distribution, as seen in the changing von Mises stress values. Near the bottom, where the temperature is highest, the material experiences significant expansion, leading to higher stress.
- Material properties and constraints: The behavior of the material in response to thermal stress is influenced by its intrinsic properties, like thermal expansion coefficient, and the constraints imposed by the design. We believe that the latest factor is of lowest effect given that the cylindrical design geometry was intentionally chosen to reduce constraints. Nonetheless, this factor should not be entirely disregarded.
- Critical region of material behavior change: The specific region could signify a transition zone where the material's response to thermal stress begins to stabilize. The convergence of stress values across different temperatures suggests a reduction in the temperature gradient, leading to a more uniform distribution of thermal expansion. This could be due to the material reaching a more uniform temperature along the height of the cylinder, or it could indicate a region where the material's inherent properties or structural constraints change, altering how it responds to the thermal load.

In summary, the observed shift in stress patterns and performance characteristics at a specific region from the cylinder's bottom surface is indicative of the complex interplay between thermal gradients, material properties, and design constraints. This understanding is crucial for the effective application of the material in environments where it is subject to varying thermal conditions. The low thermal conductivity of the graphene-based aerogel (0.02 to 0.04 W/m.k) plays a pivotal role in the temperature distribution and stress patterns observed in the material. A deeper analysis of this property, along with a comparison to similar materials, can provide a more comprehensive understanding of its significance in various applications. The low thermal conductivity means that heat does not spread evenly throughout the material, and therefore, a non-uniform temperature distribution. This results in a steep temperature gradient, particularly near the heat source, leading to differential expansion across the material. Furthermore, since heat cannot dissipate quickly, areas close to the heat source experience significant thermal expansion compared to cooler areas. This differential expansion contributes to the development of localized stress zones, as evidenced by the von Mises stress analysis. Compared to similar materials such traditional silica aerogels, graphene aerogels, due to their unique structure, could offer better mechanical stability and strength under thermal stress, making them more suitable for high-stress environments. Other materials like metals have higher thermal conductivity (237 to 429 W/m.k), leading to a more uniform temperature distribution under similar conditions. In contrast, the graphene aerogel’s low thermal conductivity results in more pronounced thermal gradients and stress concentrations, advantageous in keeping heat-sensitive components protected in specific areas, preventing the

spread of heat to sensitive parts. Composite materials combine properties of different constituents, such as polymers and ceramics, might offer a balance between thermal conductivity and mechanical strength. They have a thermal conductivity range from 0.1 to 0.5 W/m.k and from 1 to 40 W/m.k, respectively. The behavior of graphene aerogels under thermal stress could be contrasted with these composites to understand the trade-offs in terms of thermal management and structural integrity. Thus, when compared with other materials, graphene aerogels present unique challenges and opportunities. This property must be carefully considered in engineering applications, particularly those requiring precise thermal management and insulation, while also while also being lightweight (aerospace applications) and accounting for mechanical stability under thermal stress. Observing and understanding the variations in stress patterns within the graphene-based aerogel is vital for design considerations, especially in high thermal stress applications. Recognizing the region where the material's performance changes enable engineers to design safer, more reliable, and efficient systems by selecting appropriate materials, designing to accommodate thermal stresses, and potentially innovating new solutions to manage these challenges without compromising safety or functionality. It is important to mention that observing such variation of stress patterns could be expected in some designs because of material properties and the geometrical design constraints. However, the more important is to get lower values of stress all over the structure. This is particularly important in applications where the material is exposed to varying thermal conditions, as overlooking such changes could lead to material failure or inefficiency. Some concrete examples can be mentioned in several applications such like:

- Spacecraft heat shields in aerospace engineering applications, where understanding how thermal stress evolves, and stress patterns concentration could guide the selection of materials and structural designs that resist thermal fatigue and prevent failure during critical phases of flight.
- Engine blocks or exhaust systems in automotive Industry applications where the varying stress patterns observed near the heat source could inform the design of these components and the best material insuring higher thermal resistance to prevent deformation or failure under extreme conditions.
- Heat sinks or other cooling mechanisms designs in electronic and microchip fabrication applications where analysis and measurement of stress distribution patterns in materials is crucial for maintaining functionality and prolonging the lifespan of the device, as excessive heat can lead to component failure.
- Many other examples such as engine blocks or exhaust systems in automotive Industry applications, nuclear reactors, or solar thermal plants in energy sector applications, etc.

5. CONCLUSION

In conclusion, our comprehensive study using COMSOL Multiphysics simulations has provided significant insights into the thermal and mechanical properties of Ethylenediamine Graphene Aerogel (EGA) material. The findings highlight EGA's unique response to thermal stress, particularly its behavior under varying temperature conditions, which is crucial for its application in diverse engineering fields. The study presents a sequential analysis of stress distribution in a graphene-based aerogel cylinder over different time intervals (0, 20, and 40 minutes). It reveals a significant progression in the distribution of Von-Mises equivalent

stress, which initially is uniform but increases steadily over time due to heat applied at the cylinder's lower surface. This increase in stress is largely due to uneven thermal expansion within the material. By the 40-minute mark, the stress levels start to stabilize, suggesting the material reaches a new thermal equilibrium. Higher stress concentrations are observed near the heat source, while areas farther away experience lower stress levels. This behavior highlights the material's thermal response, including expansion and the influence of internal constraints. Notably, a critical area near the bottom surface exhibits a marked shift in stress patterns, attributed to the material's low thermal conductivity, leading to substantial thermal gradients, uneven thermal expansion, and localized stress zones. These observations are crucial for understanding the behavior of Ethylenediamine Graphene Aerogel (EGA) under varying thermal conditions and stresses. Compared to other materials, such as traditional silica aerogels or metals with higher thermal conductivity, EGA presents a unique combination of low thermal conductivity with improved mechanical stability. This balance is beneficial in applications requiring precise thermal management and insulation, especially where lightweight and mechanical stability are crucial, such as in aerospace, automotive, and electronic industries. Our study not only validates the use of numerical simulations for predicting the behavior of advanced materials like EGA but also opens up new avenues for their application. The insights gained are valuable for the scientific and engineering community, providing a deeper understanding of how material properties like thermal conductivity and mechanical behavior under stress can influence design and functionality. This knowledge is instrumental in guiding material selection and structural design in high thermal stress environments, ensuring safety, efficiency, and reliability in various technological applications. The findings from this study thus make a significant contribution to the ongoing research and development in the field of advanced material sciences and engineering.

REFERENCES

[1] Y. Lu, X. Li, X. Yin, H. D. Utomo, N. F. Tao, and H. Huang, “Silica Aerogel as Super Thermal and Acoustic Insulation Materials,” J Environ Prot (Irvine, Calif), vol. 09, no. 04, 2018.

[2] Y. Xu, K. Sheng, C. Li, and G. Shi, “Self-assembled graphene hydrogel via a one-step hydrothermal process,” ACS Nano, vol. 4, no. 7, 2010.

[3] R. Ma et al., “Multidimensional graphene structures and beyond: Unique properties, syntheses and applications,” Progress in Materials Science, vol. 113. 2020.

[4] C. I. L. Justino, A. R. Gomes, A. C. Freitas, A. C. Duarte, and T. A. P. Rocha-Santos, “Graphene based sensors and biosensors,” TrAC - Trends in Analytical Chemistry, vol. 91. 2017.

[5] S. Kumar et al., “Electrochemical Sensors and Biosensors Based on Graphene Functionalized with Metal Oxide Nanostructures for Healthcare Applications,” ChemistrySelect, vol. 4, no. 18. 2019.

[6] V. Jain and B. Kandasubramanian, “Functionalized graphene materials for hydrogen storage,” Journal of Materials Science, vol. 55, no. 5. 2020.

[7] X. Zhao et al., “A review of studies using graphenes in energy conversion, energy storage and heat transfer development,” Energy Conversion and Management, vol. 184. 2019.

[8] A. G. Olabi, M. A. Abdelkareem, T. Wilberforce, and E. T. Sayed, "Application of graphene in energy storage device – A review," Renewable and Sustainable Energy Reviews, vol. 135. 2021.

[9] S. K. Tiwari, V. Kumar, A. Huczko, R. Oraon, A. De Adhikari, and G. C. Nayak, "Magical Allotropes of Carbon: Prospects and Applications," Critical Reviews in Solid State and Materials Sciences, vol. 41, no. 4. 2016.

[10] S. Araby, A. Qiu, R. Wang, Z. Zhao, C. H. Wang, and J. Ma, "Aerogels based on carbon nanomaterials," Journal of Materials Science, vol. 51, no. 20. 2016.

[11] B. Singh and M. Dhiman, "Carbon aerogels for environmental remediation," in Advances in Aerogel Composites for Environmental Remediation, 2021.

[12] [12] Z. S. Wu, S. Yang, Y. Sun, K. Parvez, X. Feng, and K. Müllen, "3D nitrogen-doped graphene aerogel-supported Fe 3O 4 nanoparticles as efficient electrocatalysts for the oxygen reduction reaction," J Am Chem Soc, vol. 134, no. 22, 2012.

[13] [13] V. Deerattrakul, P. Puengampholsrisook, W. Limphirat, and P. Kongkachuichay, "Characterization of supported Cu-Zn/graphene aerogel catalyst for direct CO2 hydrogenation to methanol: Effect of hydrothermal temperature on graphene aerogel synthesis," Catal Today, vol. 314, 2018.

[14] [14] M. Kotal, J. Kim, J. Oh, and I. K. Oh, "Recent progress in multifunctional graphene aerogels," Frontiers in Materials, vol. 3. 2016.

[15] [15] M. A. Worsley, P. J. Pauzauskie, T. Y. Olson, J. Biener, J. H. Satcher, and T. F. Baumann, "Synthesis of graphene aerogel with high electrical conductivity," J Am Chem Soc, vol. 132, no. 40, 2010.

[16] [16] Z. Wang et al., "Ultralight, highly compressible and fire-retardant graphene aerogel with self-adjustable electromagnetic wave absorption," Carbon N Y, vol. 139, 2018.

[17] [17] H. Hu, Z. Zhao, W. Wan, Y. Gogotsi, and J. Qiu, "Ultralight and highly compressible graphene aerogels," Advanced Materials, vol. 25, no. 15, 2013.

[18] [18] J. Li et al., "Ultra-light, compressible and fire-resistant graphene aerogel as a highly efficient and recyclable absorbent for organic liquids," J Mater Chem A Mater, vol. 2, no. 9, 2014.

[19] [19] C. Li, L. Qiu, B. Zhang, D. Li, and C. Y. Liu, "Robust Vacuum-/Air-Dried Graphene Aerogels and Fast Recoverable Shape-Memory Hybrid Foams," Advanced Materials, vol. 28, no. 7, 2016.

[20] [20] G. Zu et al., "Superelastic Multifunctional Aminosilane-Crosslinked Graphene Aerogels for High Thermal Insulation, Three-Component Separation, and Strain/Pressure-Sensing Arrays," ACS Appl Mater Interfaces, vol. 11, no. 46, 2019.

[21] [21] Q. Han, L. Yang, Q. Liang, and M. Ding, "Three-dimensional hierarchical porous graphene aerogel for efficient adsorption and preconcentration of chemical warfare agents," Carbon N Y, vol. 122, 2017.

[22] [22] S. Tang et al., "Dye adsorption by self-recoverable, adjustable amphiphilic graphene aerogel," J Colloid Interface Sci, vol. 554, 2019.

[23] [23] S. Dong et al., "Controlled synthesis of flexible graphene aerogels macroscopic monolith as versatile agents for wastewater treatment," Appl Surf Sci, vol. 445, 2018.

[24] [24] C. Wang, S. Yang, Q. Ma, X. Jia, and P. C. Ma, "Preparation of carbon nanotubes/graphene hybrid aerogel and its application for the adsorption of organic compounds," Carbon N Y, vol. 118, 2017.

[25] M. Hasanpour and M. Hatami, "Application of three dimensional porous aerogels as adsorbent for removal of heavy metal ions from water/wastewater: A review study," Advances in Colloid and Interface Science, vol. 284. 2020.

[26] G. Nassar, S. Youssef, and R. Habchi, "Nitrogen-doped graphene aerogels for highly efficient toluene removal from water," Graphene and 2D Materials, vol. 7, no. 1–2, 2022.

[27] M. H. Tavakoli Dastjerdi, G. Habibagahi, A. Ghahramani, A. Karimi-Jashni, and S. Zeinali, "Removal of dissolved toluene in underground water with nanowires of manganese oxide," Adsorption Science and Technology, vol. 36, no. 1–2, 2018.

[28] T. AlZoubi, B. Mourched, M. Al Gharram, G. Makhadmeh, and O. Abu Noqta, "Improving Photovoltaic Performance of Hybrid Organic-Inorganic MAGeI3 Perovskite Solar Cells via Numerical Optimization of Carrier Transport Materials (HTLs/ETLs)," Nanomaterials, vol. 13, no. 15, 2023.

[29] B. Mourched, S. Sawaya, M. Abdallah, and N. Abboud, "Effect of Buffer Layer selection on Perovskite-Based Solar Cell Efficiency: A Simulation Study Using OghmaNano Software," International Journal of Multiphysics, vol. 17, no. 2, 2023.

[30] B. Mourched, N. Abboud, M. Abdallah, and M. Moustafa, "Electro-Thermal simulation study of MOSFET modeling in Silicon and Silicon carbide," International Journal of Multiphysics, vol. 16, no. 4, 2022.

[31] B. Mourched and M. Abdallah, "Design and characterization of a new microscopy probe using COMSOL and ANSYS," International Journal of Multiphysics, vol. 16, no. 1, 2022.

[32] B. Qi et al., "Experimental and Numerical Investigation of Temperature Development of Ohmic Heating Cured Nonmass Concrete under Subzero Temperature," Advances in Civil Engineering, vol. 2021, 2021.

[33] Y. Liu and X. Huang, "Effects of flash sintering parameters on performance of ceramic insulator†," Energies (Basel), vol. 14, no. 4, 2021.

[34] A. Laouar and D. Omeiri, "Parametric study with simulation of transport phenomenon of a solid oxide fuel cell," International Journal of Multiphysics, vol. 13, no. 4, 2019.

[35] S. Chugh, S. Ghosh, A. Gulistan, and B. M. A. Rahman, "Machine Learning Regression Approach to the Nanophotonic Waveguide Analyses," Journal of Lightwave Technology, vol. 37, no. 24, 2019.

[36] B. Mourched et al., "Piezoelectric-Based Sensor Concept and Design with Machine Learning-Enabled Using COMSOL Multiphysics," Applied Sciences (Switzerland), vol. 12, no. 19, 2022.

[37] B. Mourched, M. Abdallah, M. Hoxha, and S. Vrtagic, "Machine-Learning-Based Sensor Design for Water Salinity Prediction: A Conceptual Approach," Sustainability (Switzerland), vol. 15, no. 14, 2023.

[38] W. Hao, Y. Huang, and G. Zhao, "Acoustic sources localization for composite pate using arrival time and BP neural network," Polym Test, vol. 115, 2022.

[39] U. Demircioğlu, A. Sayil, and H. Bakır, "Detecting Cutout Shape and Predicting Its Location in Sandwich Structures Using Free Vibration Analysis and Tuned Machine-Learning Algorithms," Arab J Sci Eng, 2023.